Analysis of backscattered ultrasound amplitude of Ti–5.8Al–4Sn–3.5Zr–0.7Nb–0.5Mo–0.3Si samples in terms of their microstructures and local textures

Humbert, M.; Moreau, A.; Uta, E.; Gey, N.; Bocher, P.; Bescond, C.

Publisher's version / Version de l'éditeur:
https://doi.org/10.1016/j.actamat.2008.10.012
Acta Materialia, 57, 3, pp. 708-714, 2009-02

Available online at www.sciencedirect.com
ScienceDirect
Acta Materialia 57 (2009) 708–714
Acta MATERIALIA
www.elsevier.com/locate/actamat

Analysis of backscattered ultrasound amplitude of Ti–5.8Al–4Sn–3.5Zr–0.7Nb–0.5Mo–0.3Si samples in terms of their microstructures and local textures

M. Humbert [a,*], A. Moreau [b], E. Uta [a], N. Gey [a], P. Bocher [c], C. Bescond [b]

[a] *Laboratoire d'Etude des Textures et Applications aux Matériaux, LETAM, CNRS UMR 7078, Université de Metz, F-57045 Metz Cedex 01, France*
[b] *Industrial Materials Institute, National Research Council of Canada, 75 de Mortagne Blvd., Boucherville, Que., Canada J4B 6Y4*
[c] *École de technologie supérieure, Montréal, Que., Canada*

Received 24 July 2008; received in revised form 1 October 2008; accepted 9 October 2008
Available online 18 November 2008

Abstract

The amplitudes of backscattered ultrasound were measured at 10 MHz on different samples of the near-α titanium alloy Ti–5.8Al–4Sn–3.5Zr–0.7Nb–0.5Mo–0.3Si. Orientation imaging maps (OIMs) of these samples were also determined by electron backscatter diffraction. The backscattered amplitude appears to be related to the microstructure, notably to the orientations, volume fractions and spatial distribution of specific zones. These zones, named macrozones, are formed with a majority of primary α_p grains and secondary α_s colonies having nearly a common crystallographic axis. To illustrate the role of the microstructure on wave propagation, the local elastic constants determining the velocities of the longitudinal ultrasonic waves were deduced from the OIMs. The analysis of the spatial distribution and variations of the elastic constants explains the observed variations in backscattered ultrasound amplitude.

Keywords: IMI 834; Texture heterogeneities; EBSD; Backscattered ultrasound

1. Introduction

The titanium alloy Ti–5.8Al–4Sn–3.5Zr–0.7Nb–0.5Mo–0.3Si, also called IMI 834, is a near-α titanium alloy used for rotating engine components. Through processing, it acquires a bimodal microstructure consisting of primary, α_p, grains and secondary, α_s, colonies inherited from β grains. This bimodal microstructure is designed for improved mechanical properties such as high fatigue and creep resistance for service temperatures up to 600 °C [1]. A billet is first machined from a cast ingot, then forged in the α–β field to obtain a reduced diameter. The resulting microstructure contains elongated zones, named macrozones, which are elongated in the axial direction of the billet. In these macrozones the α_p and α_s grains have preferred crystallographic orientations linked in a complex way to the orientations of the deformed primary α_p grains and of the deformed β grains present in the α–β field [2–4]. Because the changes of compression direction in the forging process induce inhomogeneous local stresses and strains in the billet, after several steps the orientation couplings finally weaken and many volumes lose their macrozone character. Nevertheless, some of these volumes retain this character. These heterogeneities can cause a significant decrease of creep and fatigue performance, leading to a great reduction in the service life of the product, notably by dwell [5].

A precise study of the macrozones, whose sizes are of the order of millimeters, can be performed by scanning electron microscopy (SEM) and electron backscattering diffraction (EBSD) to obtain their microstructural characteristics [6–8]. However, these techniques, whose principal role is local investigations, are not well adapted for efficient

* Corresponding author. Tel.: +33 38731 5387; fax: +33 38731 5370.
E-mail address: michel.humbert@univ-metz.fr (M. Humbert).

1359-6454/$34.00 © 2008 Acta Materialia Inc. Published by Elsevier Ltd. All rights reserved.
doi:10.1016/j.actamat.2008.10.012

detection of the macrozones as these can be large compared to the scanned area.

Because many titanium alloy single crystals (like IMI 834) are elastically anisotropic, ultrasonic volume inspection is sensitive to local crystallographic orientations and more generally to the sample microstructure. Notably, attenuation of the ultrasound amplitude, the backscattered ultrasound amplitude (i.e. the amplitude of the ultrasound scattered backwards), and the velocity of sound depend on the microstructure. For example, it was found very early that in a Ti–5Al–6V–2Sn alloy ultrasound waves were backscattered from α colonies of similar crystallographic orientations and that the backscattered intensity was highest when the sound beam was perpendicular to large planar boundaries [9]. This backscattered amplitude could cause the false detection of defects [9] or seriously degrade the ability to image flat-bottomed holes in Ti-6242 [10].

The behaviour of ultrasound in microstructures consisting of grains and colonies has been studied from various points of views. Detailed scattering models were made [11–15] and showed that in the two-phase alloy Ti–6Al–4V the backscattered ultrasound amplitude is large in directions perpendicular to the elongated macrozones, and weak in the direction of the elongated macrozones. Ultrasonic attenuation was found to be highest in the direction of the elongated macrozones. This was attributed to phase shifts caused by the elongated macrozones [16,17]. Furthermore, EBSD measurements in a Ti–6Al–4V alloy showed that regions with high and low backscattered amplitudes in a single part were associated with different microtextures caused by thermomechanical processing [18,19]. These microtextures could also explain backscattered signal anisotropy as well as ultrasonic attenuation anisotropy. Finally, it was shown recently that the backscattered ultrasound amplitude can be dissimilar in different regions of a single forged part [20].

In this paper, two samples taken from a single forged cylindrical billet made from the near-α alloy IMI 834 are compared ultrasonically and by EBSD. The two samples are taken from two geometrically equivalent positions and should be similar. However, when ultrasound is propagated in the direction perpendicular to the macrozones, i.e. in the direction of high backscattering amplitude, one sample has a high backscattered signal amplitude while the other one has a low amplitude. The texture characteristics of both samples are determined by EBSD and utilized to explain the differences observed by ultrasonics.

2. Materials and methods

2.1. Samples

The investigated IMI 834 disk was acquired from an initial ingot and its processing resulted in a microstructure consisting of approximately 30% equiaxed α_p grains surrounded by lamellar α_s laths with thin β layers between α_s laths. The equiaxed α_p grain size is about 25 μm, whereas the width of the α_s laths is around 2 μm.

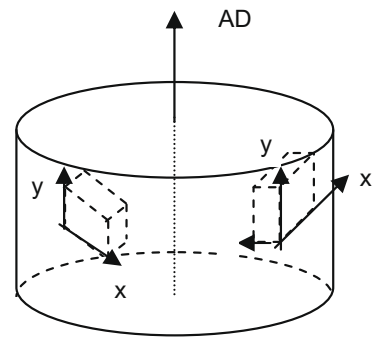

Fig. 1. Parallelepiped localizations in the IMI 834 disk. AD is the axial direction. EBSD investigations are performed on the *x–y* planes. The *x*, *y* and *z* axes are parallel to the tangential, axial and the negative of the radial directions, respectively.

Two large parallelepipeds referred to as HBA (high backscattered amplitude sample) and LBA (low backscattered amplitude sample) ($l \times h \times d = 90 \times 30 \times 20$ mm) were cut from two different locations in the IMI 834 disk (Fig. 1).

2.2. EBSD analysis

Several EBSD scans of an area of some millimeters (12.5 × 7.5 mm) with a step size of 15 μm were performed on face 1 (*x–y*) of the samples in a 6500F JEOL field emission gun-scanning electron microscope equipped with a Channel 5 system (HKL technology, Denmark). The choice of face 1 ($l \times h = 90 \times 30$ mm) for EBSD investigations was dictated by the fact that texture heterogeneities develop in specific and limited disk sectors and form volumes elongated in the axial direction. The resulting orientation imaging maps (OIMs) are representative of the large face 1 and contain the orientation of each diffraction location on the *x–y* plane of the samples. Generally, in the OIMs, a colour key is used to display information about the local orientations [2,3,6]. However, in this contribution, we exhibit some specific characteristics of the microstructure calculated from the OIMs. Fig. 2 is a representative example. Fig. 2a (respectively Fig. 2c) shows the locations in sample HBA (resp. sample LBA) where the *c* axes of the hexagonal close-packed (hcp) α grains are oriented in the *x* direction with a tolerance angle of 20°. Fig. 2b (respectively Fig. 2d) indicates the locations in sample HBA (resp. sample LBA) where the *c* axes are perpendicular to the *x* direction with the same tolerance.

Sample HBA (Fig. 2) displays a succession of two types of bands, elongated in the *y* direction (perpendicular to *x*). The first ones (Fig. 2a) are well identified by the high density of black points (8% of the total points of the map) with *c* axes parallel to the *x* direction. The other bands between the first ones contain points (35%) whose *c* axes are perpendicular to *x* (in black in Fig. 2b). The remaining 57% of points have the *c* axes neither parallel to *x* nor perpendicular to *x*. The bands of Fig. 2a, characterized by a majority of grains with com-

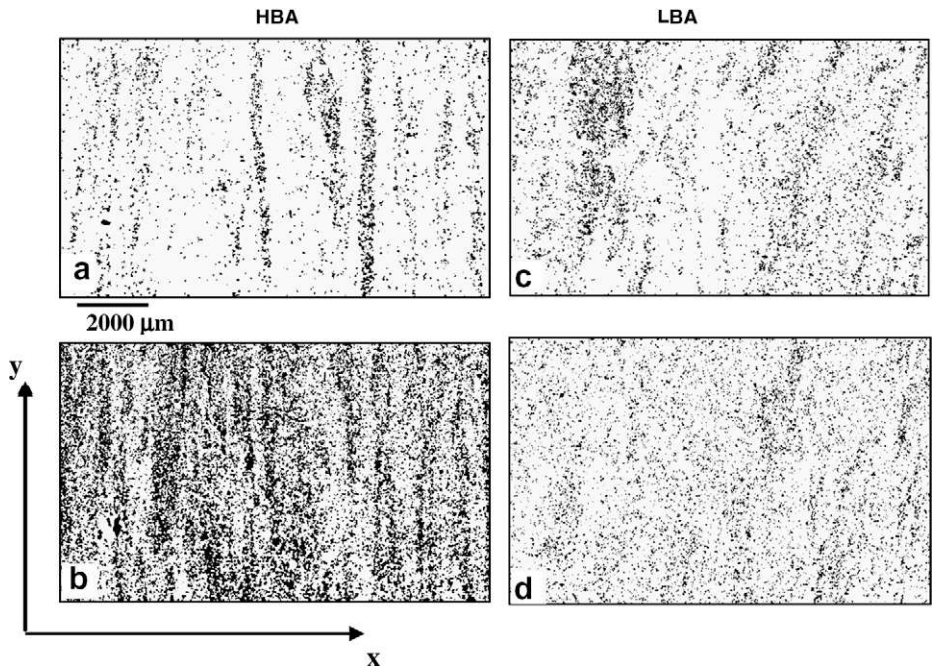

Fig. 2. Orientation maps of samples HBA (a and b) and LBA (c and d). The black points indicate the locations where the *c* axes are parallel to x (a and c) and where the *c* axes are perpendicular to x (b and d) with a tolerance of 20°.

mon *c* axes (black points) in the *x* direction, define a particular type of macrozone. The situation is very different for sample LBA which does not present such somewhat periodic and regular bands, neither for *c* axes parallel to *x* (Fig. 2c) (10.7% of the total points) nor perpendicular to *x* (Fig. 2d) (23% of the total points). In this case, with a tolerance angle of 20°, more points (66.3%) than for HBA have *c* axes neither parallel to *x* nor perpendicular to *x*. These different percentages show that the sharpness of the local texture differs for LBA and HBA as more specific texture studies can attest [21]. These various local orientation distributions according to the samples suggest that the deformation field during forging within the Ti disk was very inhomogeneous so that it led to different local microstructures.

2.3. Ultrasound investigations

The amplitude of the backscattered ultrasound was measured as follows. A sample was immersed in water. A wideband, 10 MHz, unfocused ultrasonic transducer was also immersed and oriented so that the ultrasound propagated in water in a direction normal to one of the two smallest, (*y*–*z*), sample surfaces (see Fig. 1). A short pulse of ultrasound was excited electrically. The pulse propagated to the water–sample interface, into the sample and to the opposite side (the opposite sample–water interface) where it was reflected back along the same path all the way to the transducer. Along the way, some of the pulse energy was also reflected back at the first water–sample interface and by the internal microstructure of the sample. The measurement was repeated for each of the two *y*–*z* surfaces of the two samples.

Fig. 3 shows the detected signal amplitude obtained on both samples. The large signal amplitude shown at the beginning and at the end of the figures (0 and 30 μs), respectively, are much larger than the vertical scale of the diagram. They correspond to the wave reflection at the two water–sample interfaces, 90 mm apart. The ultrasound backscattered by the microstructure is shown in between the two reflections. The portion between 5 and 25 μs was selected and its mean root mean squared (RMS) amplitude measured. The vertical scale shown in mV depends on amplifier gains and transducer characteristics. Those units can be considered arbitrary, but because the measurement conditions were identical for all measurements, all measurements can be compared relative to each other.

The backscattered signal amplitude in the intermediate time interval (5–25 μs) was of 47.5 mV RMS for sample HBA and 22.5 mV RMS for sample LBA. Thus, the RMS amplitude is approximately twice as large for HBA. Interchanging sample sides led to similar results.

3. Discussion

In polycrystalline materials, the attenuation of ultrasonic waves and the amplitude of the backscattered noise depend on the elastic properties of the grains, on their orientations, on their size, *D*, and on ultrasonic wavelength, λ. With a wavelength of about 0.6 mm in Ti at an ultrasonic frequency of 10 MHz and with a 25 μm size of the individual α_p grains (2 μm for the α_s grains) in both samples the difference in the backscattered noise amplitudes in samples HBA and LBA cannot be explained easily by scattering from individual α_p (or α_s) grains because these grains are

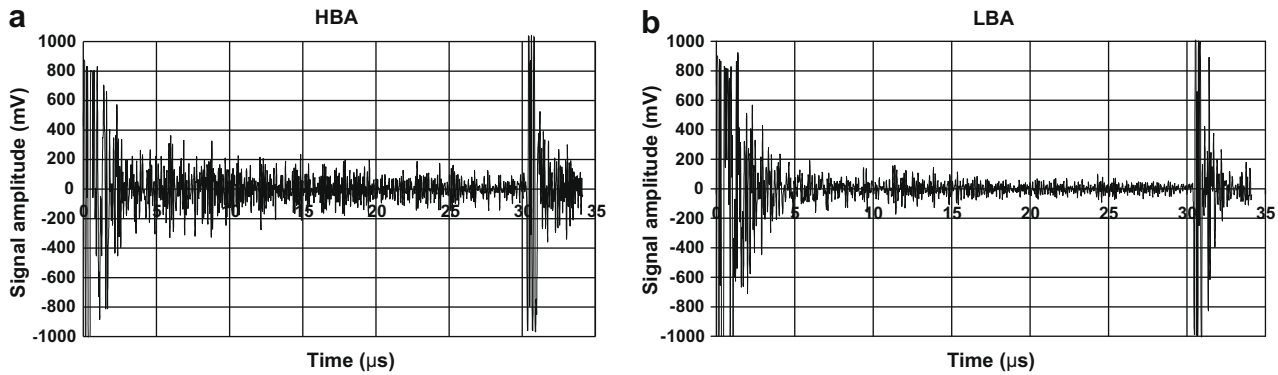

Fig. 3. Detected ultrasonic amplitude measured at 10 MHz on samples HBA (a) and LBA (b).

so small that very little backscattering would be expected and because these grains have the same dimensions and volume fractions in both samples.

The main difference is, in sample HBA, the marked presence of parallel bands, periodically distributed, normal to x, with a high density of α_p and α_s grains having their c axes along x for one band type and perpendicular to x for the other band type. These features extend several millimeters in the y direction and up to a few millimeters in the x direction. They are relatively homogeneous and could contribute to backscattering because they are much larger than individual grains and of dimensions comparable to or even exceeding λ. Theses bands are less pronounced in sample LBA and would be expected to contribute less. The observed bands correspond to different textures and, consequently, to differences in local elastic behaviour.

Due to the anisotropy of the elastic constants of the Ti single crystal, the longitudinal wave velocity decreases from $\sqrt{\frac{C_{33}}{\rho}}$ along the c axis to $\sqrt{\frac{C_{11}}{\rho}}$ in the basal plane of the crystal, i.e. from 6332 to 6003 m s^{-1}, considering the elastic constants of Ti single crystal ($C^{\alpha}_{11} = 1.624$, $C^{\alpha}_{33} = 1.807$, $C^{\alpha}_{12} = 0.920$, $C^{\alpha}_{13} = 0.690$, $C^{\alpha}_{44} = 0.467 \times 10^5$ MPa [22]) and its density ($\rho = 4507$ kg m^{-3}). By considering the texture and the anisotropy of the elastic constants, the mean velocity of the longitudinal waves propagating along x were calculated for both samples. We obtained 6083 and 6093 m s^{-1} for HBA and LBA samples, respectively. Therefore, the two samples appear nearly indistinguishable from a bulk perspective. However, although the difference in mean velocity is small, 10 m s^{-1}, the variation of the wave velocity as a function of location within the sample can be as high as 329 m s^{-1} for ideal orientations. This suggests that the backscattering amplitude difference between the two samples could be linked to differences in local elastic behaviours and notably to local variations in the acoustic velocities.

We now present two models to develop these ideas and explain the different backscattering response of the two samples. The first model is somewhat simplistic, but provides a good qualitative understanding of the mechanisms responsible for the difference in backscattered amplitude. The second model is based on recent models proposed in the literature and provides quantitative predictions.

3.1. Qualitative approach

At the boundary between two media (1 and 2) with different acoustical impedances, a part of the incident wave is reflected. The reflection coefficient r is related to the acoustic impedances $Z = \sqrt{\rho V_L}$ of both media by:

$$r = \left(\frac{Z_2 - Z_1}{Z_2 + Z_1}\right)^2 = \left(\frac{\sqrt{\rho V_{L2}} - \sqrt{\rho V_{L1}}}{\sqrt{\rho V_{L2}} + \sqrt{\rho V_{L1}}}\right)^2,$$

where ρ is the density and V_L the local velocity of the longitudinal waves. Therefore the backscattered ultrasound amplitude should be larger in materials presenting larger variations in acoustic impedance and velocity. In addition, for materials having inhomogeneous microstructures such as this IMI 834 alloy, the backscattered ultrasound intensity should be stronger in the directions having large and sharp variations in acoustic impedance and velocity. Clearly, the larger the magnitude, the larger the scattering. However, the length scale over which these variations occur is also important. If these variations occur over a length scale that is very short compared to the acoustic wavelength, then the material will be acoustically homogeneous and scattering will be very small. However, if these variations occur over a length scale comparable to or shorter than that of the acoustic wavelength, then scattering will be much stronger.

The backscattered ultrasound intensity was measured in the x direction. Therefore we attempted to compare the velocity variations in the x direction for the two samples. The velocity $V_L(x,y) = \sqrt{\frac{c_{11}}{\rho}}$ is calculated from the crystallographic orientation at each location on the OIM, from the elastic constants of Ti single crystal and from its density ρ. By inspection of Fig. 2, one can see that the macrozones form vertical bands that are relatively uniform and well aligned in the y direction, so the obtained velocities were averaged in the y direction. We obtained the mean velocity of the waves travelling in the x direction $\overline{V_L(x)} = \frac{1}{y_{Max}} \int_0^{y_{Max}} V_L(x,y)\mathrm{d}y$ as a function of x. Fig. 4 shows the results for both samples at the same scale as in Fig. 2.

For the HBA sample (Fig. 4a), $\overline{V_L(x)}$ shows large (of the order of 100 m s^{-1}) and sharp (over a distance of the order of 100 μm) changes in velocity. These sharp changes are separated by distances of the order of 0.5 to several millimeters, in concordance with the bands perpendicular to the x direction in Fig. 2a. The highest velocities correspond to the bands formed of black points (with the c axis of the crystal parallel to x). In contrast, the LBA sample (Fig. 4b) has small velocity variations, of the order of less than 50 m s^{-1}, occurring over short distances, with only one clearly visible structure (~2 mm). This observation leads us to hypothesize that the stronger backscattered signal in the HBA sample is caused by those bands of sharply varying acoustic impedance.

3.2. Quantitative approach

A number of fundamental works have been devoted to ultrasonic scattering and elastic heterogeneities (see notably Refs. [23,24]). Among them, we adopted a model proposed by Rose [12] to sustain a quantitative interpretation of the present experimental results. In the notation of Han and Thompson [14], the model predicts that the backscattered power is proportional to

$$\chi^2(2k) = \int \langle \delta C_{11}(r)\delta C_{11}(r')\rangle \exp(2ik(r-r'))\mathrm{d}^3(r-r'),$$

where δC expresses the difference between an elastic constant C_{ij} and its mean value. The quantity $\langle \delta C_{11}(r)\delta C_{11}(r')\rangle$ which represents the ensemble average, is displayed with respect to the shift, $r - r' = h$ in the x direction, in Fig. 5 for both samples. Both autocorrelation functions show a peak near zero. This peak shows that as the distance increases between two points it is less likely that the elastic constants are the same. For the LBA sample, beyond 2 mm, the probability that two points have the same elastic constants is close to zero. For the HBA sample, however, the function is nearly periodic with a period of ~1 mm. This reflects the spacing between the bands described previously. It is worth noting that such a periodic behaviour does not appear to have been noted or modelled by previous authors concerned with ultrasonic measurements.

The backscattered power, $\chi^2(2k)$, is essentially the Fourier transform of $\langle \delta C_{11}(r)\delta C_{11}(r')\rangle$, where k is equal to $2\pi/\lambda$ and λ is the wavelength. $\chi^2(2k)$ is shown in Fig. 6. Clearly, the backscattered power is predicted to fluctuate widely with frequency in the HBA sample, and it is expected to be larger on average. In the frequency range of 5 MHz ($2k = 11$ mm^{-1}) to 15 MHz ($2k = 31$ mm^{-1}),

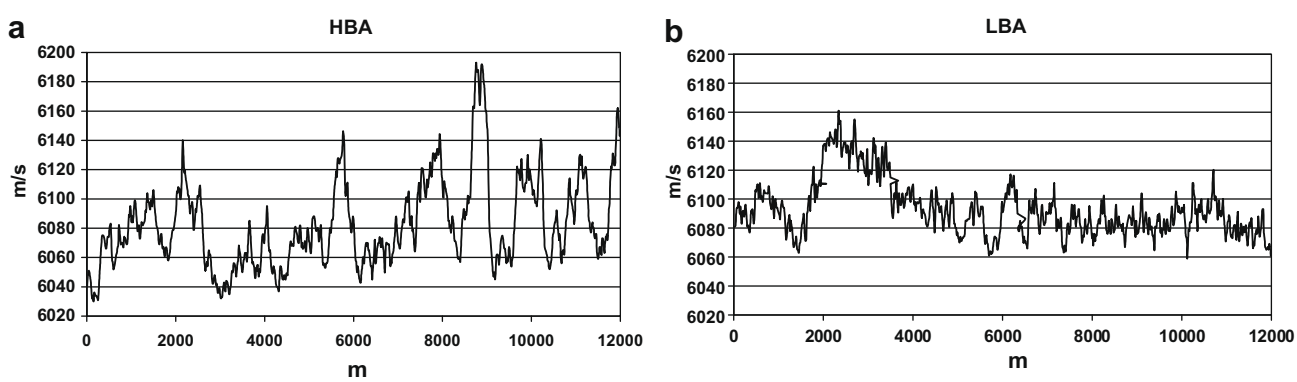

Fig. 4. Expected mean velocities for longitudinal waves calculated from the IOMs of samples HBA (a) and LBA (b).

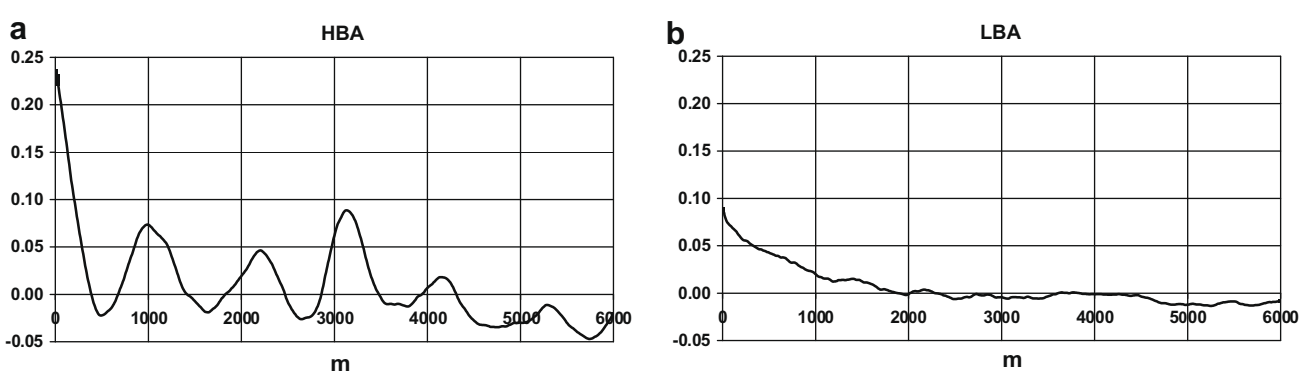

Fig. 5. Spatial correlation function $\langle \delta C_{11}(r)\delta C_{11}(r')\rangle$ with respect to distance h between two points along the propagation direction for samples HBA (a) and LBA (b).

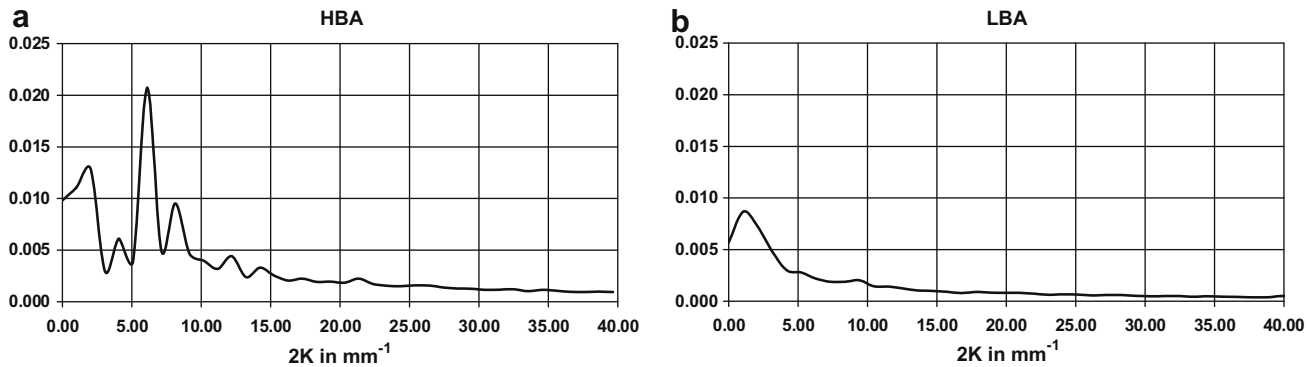

Fig. 6. $\chi^2(2k)$ (Fourier transform of $\langle \delta C_{11}(r)\delta C_{11}(r')\rangle$) in function of 2k, for samples HBA (a) and LBA (b).

which is approximately the bandwidth of the transducer, the mean value of $\chi^2(2k)$ is ~2.6 times as large as in the HBA sample. Since the amplitude is proportional to χ, the square root of factor 2.6 ($\sqrt{2.6} = 1.6$) should be equal to the measured RMS amplitude ratio, which is equal to 2.1. The difference of 25% between these two quantities is not negligible but remains limited considering the experimental errors. Notably the small surface (6×12 mm) of the sample used for microstructural investigations might not be completely representative of the heterogeneities of the whole volume used for the ultrasonic tests.

These different features suggest that the difference in amplitudes of the backscattered noise measured in samples LBA and HBA is linked to the local variations of the elastic constants in the x direction. Indeed, in sample HBA these variations are more numerous, of higher amplitude and occur over characteristic distances that approach that of the acoustic wavelength. As a consequence, the observed backscattered ultrasound amplitude of the HBA sample is twice as high as that of the LBA sample. In addition, the HBA sample appears to have quasi-periodic structures that enhance backscattering at some frequencies.

4. Conclusion

This work concerns the analysis of the ultrasonic responses in IMI 834, and how these correlate with heterogeneities in the local texture. The two selected samples present strong and weak ultrasonic backscattered amplitudes, respectively. EBSD measurements reveal the presence of macrozones in the two samples. However, in the sample with a weak ultrasonic backscattered amplitude, the macrozones are not as sharply defined and clearly observed. The amplitude difference is not explained by the size of the grains, which are the same in both samples. The higher backscattered amplitude of sample HBA is associated with the presence of numerous macrozones elongated perpendicularly to the wave propagation direction. With a thickness of about one wavelength at 10 MHz, each particular macrozone behaves as a relatively uniform volume in which the wave velocity is relatively constant but different from that of its adjacent macrozones. Notably, in a macrozone, the propagation velocity in some direction is higher if the density of c-axes is higher in this direction. These features suggest that the high backscattered amplitude measured in sample HBA is linked to the sharper, larger and more frequent variations of the velocity in the x direction and which have characteristic length scales of the order of the acoustic wavelength. Consequently this leads to more backscattering of the incident ultrasonic beam in sample HBA than in sample LBA. This qualitative model is supported by a quantitative estimate of the intensity of the backscattered ultrasound amplitude using scattering models based on spatial autocorrelation of the elastic constants. The autocorrelation function was calculated from the EBSD data and the model calculation predicts that the HBA sample should be 1.6 times as "noisy" as the LBA sample, which is a value close to the experimental measurement. Moreover, both the EBSD and the ultrasonic data show that quasiperiodic macrostructures may exist in the IMI 834 alloy. These macrostructures are characterized by bands having preferred crystallographic orientations and different average elastic properties.

References

[1] Neal DF. In: Proceedings of the 6th world conference on titanium, France, 1988. p. 253.
[2] Germain L. Ph.D. thesis, University of Metz, 2005.
[3] Bridier F. Ph.D. thesis, University of Poitiers, 2006.
[4] Le Biavant Guerrier K. Ph.D. thesis, Ecole Centrale de Paris, 2000.
[5] Bache MR, Cope M, Davies HM, Evans WJ, Harrison G. Int J Fatigue 1997;19(Suppl.):S83.
[6] Germain L, Gey N, Humbert M, Bocher P, Jahazi M. Acta Mater 2005;53:3535.
[7] Sinha V, Spowart JE, Mills MJ, Williams JC. Metall Mater Trans A 2006;37A:1507.
[8] Woodfield AP, Gorman MD, Corderman RR, Sutliff JA, Yamrom B. In: Proceedings of the 8th world conference on titanium, UK, 1995. p. 1116.
[9] Ginty B, Hallam P, Hammond C, Jackson G, Robb C. In: Proceedings of the 4th world conference on titanium, Japan. Warrendale, PA: TMS-AIME; 1980. p. 2095.
[10] Gigliotti MFX, Bewplay BW, Deaton JB, Gilmore RSGA, Salichef GA. Metall Mater Trans A 2000;31A:2119.

[11] Rose JH. In: Thompson O, Chimenti DE, editors. Review of progress in quantitative non destructive evaluation, vol. 10. New York: Plenum Press; 1991. p. 715.
[12] Rose JH. In: Thompson O, Chimenti DE, editors. Review of progress in quantitative non destructive evaluation, vol. 12. New York: Plenum Press; 1992. p. 1677.
[13] Rose JH. In: Thompson O, Chimenti DE, editors. Review of progress in quantitative non destructive evaluation, vol. 11. New York: Plenum Press; 1991. p. 1719.
[14] Han YK, Thompson RB. In: Thompson O, Chimenti DE, editors. Review of progress in quantitative non destructive evaluation, vol. 14. New York: Plenum Press; 1995. p. 67.
[15] Han YK, Thompson RB. Metall Mater Trans A 1997;28A:91.
[16] Panetta PD, Margetan FJ, Yalda I, Thompson RB. In: Thompson O, Chimenti DE, editors. Review of progress in quantitative non destructive evaluation, vol. 15B. New York: Plenum Press; 1996. p. 1525.
[17] Blodgett MP, Eylon D. J Nondestruct Eval 2001;20:1.
[18] Panetta PD, Thompson RB, Margetan FJ. In: Thompson O, Chimenti DE, editors. Review of progress in quantitative non destructive evaluation, vol. 17A. New York: Plenum Press; 1998. p. 89.
[19] Thompson RB, Panetta P, Margetan FJ. In: Proceedings of the 43rd international SAMPE symposium, 1998. p. 1448.
[20] Bescond C, Lévesque D, Guénette JB, Monchalin JP. In: 16th WCNDT 2004 – world conference on NDT, Montréal, 2004. Published on CD-ROM and on the Internet at http://www.ndt.net/abstract/wcndt2004/678.htm.
[21] Uta E, Humbert M, Gey N, Hazotte A, Bocher P, Jahazi M. In: Proceedings of Matériaux 2006, Dijon, 2006.
[22] Fisher ES, Renken CJ. Phys Rev 1964;135:482.
[23] Stanke FE, Kino GS. J Acoust Soc AM 1984;75:681.
[24] Goebbels K. In: Sharpe RS, editor. Research in NDT IV. London: Academic Press; 1980. p. 87.